





EARTH'S PALEOMAGNETIC FIELD AND ITS CHANGES THROUGH TIME

Marcia Ernesto ^{1*}, Daniele Brandt ¹,
Daniel Ribeiro Franco ², and George Caminha-Maciel ³

¹Universidade de São Paulo - USP, Instituto de Astronomia, Geofísica e Ciências Atmosféricas - IAG, São Paulo, SP, Brazil

²Observatório Nacional - ON, Coordenação de Geofísica, Rio de Janeiro, RJ, Brazil

³Universidade Federal de Santa Catarina - UFSC, Laboratório de Geofísica Computacional, Florianópolis, SC, Brazil

*Corresponding author email: mernesto@usp.br

ABSTRACT. Paleomagnetism is the only way to access the behavior of the geomagnetic field of internal origin through geological time. Therefore, the complete description of the paleosecular variation (PSV) is fundamental for unraveling the evolution of the Earth's core. Modeling of PSV relies on observing the fluctuations in the direction and intensity of the field on the surface, the evaluation of the paleomagnetic data dispersion in different times and situations of low and high reversal rates, the kinematics of the virtual poles during reversals, and other aspects. Magneto-cyclostratigraphy is a powerful tool to constrain the age of sedimentary formations, and the recognition of patterns of magnetic variation represents a breakthrough in the development of cyclostratigraphy. This paper reviews some of the contributions to the subject of the Laboratory of Paleomagnetism at Instituto de Astronomia, Geofísica e Ciências Atmosféricas the University of São Paulo.

Keywords: geomagnetic field; secular variation; virtual geomagnetic pole kinematics; paleosecular variation modeling; spectral analysis; magneto-cyclostratigraphy.

INTRODUCTION

The behavior of the Earth's geomagnetic field (EMF) of internal origin through time is fundamental in unraveling the evolution of the Earth's core. The geomagnetic field generated in the outer core is dynamic, changing continuously in direction and intensity in a broad range of frequencies. The Sun's activity affects the magnetosphere and ionosphere, causing the EMF to vary from microseconds to tens of years. Longer time interval variations have internal causes and manifest at the Earth's surface in various ways. The EMF is a magnetic vector that varies from point to point on the surface in direction and intensity. The dipolar and non-dipolar components of this vector show different velocities and accelerations. All these

manifestations are referred to as the secular variation (SV) or the paleosecular variation (PSV), as the complete description of the SV can only be accessed by the paleomagnetic data. Therefore, paleomagnetism is fundamental for decoding the geomagnetic field in the past and its evolution.

The extreme variations in the geomagnetic field spectrum are the polarity changes. [Brunhes \(1906\)](#) first observed a magnetization nearly antiparallel to the present field. Nowadays, a worldwide reversal timescale is well established for at least Phanerozoic ([Gradstein et al., 2012](#)). The alternation of polarity recorded in a rock package is the basis of magnetostratigraphy, a powerful tool for dating sediments (e.g., [Langereis et al., 2010](#)).

Both sedimentary and volcanic rocks contain minerals from the ferromagnetic group that can retain the magnetic information induced by the ambient field. With paleomagnetic techniques, it is possible to recover the direction and intensity of the ancient magnetic field recorded in rocks and other materials (mainly ancient pottery and bricks). Sedimentary sequences are especially interesting for obtaining continuous records of magnetic parameters giving valuable contributions to the study of temporal variations of the EMF. On the other hand, successive lava flows are discontinuous records, generally with time gaps of unknown duration. Therefore, they are more helpful in investigating different aspects of the secular variation dynamics. One of the main focuses is the magnetization dispersion caused by the magnetic poles' wandering around the geographic poles ([Evans and Hove, 2007](#); [Panovska et al., 2019](#)).

The representation of the Earth's magnetic pole position at a particular time (one sedimentary layer or a magma flow) is a Virtual Geomagnetic Pole (VGP). The VGP is calculated assuming a geocentric axial dipole field (for details on the calculation, see [Butler, 1992](#)). The geocentric axial dipole (GAD) is a condition only achieved when the field is averaged over several thousands of years ([Panovska et al., 2019](#)). Paleomagnetic records from continuous sedimentary columns, mainly from lakes and oceans, are the best data source to investigate the long-term changes in the paleomagnetic field, both the secular variation and the polarity inversions, as are continuous records. Therefore, the VGP paths through time can be fully observed. However, sampling sites distant about 1000 km may give non-coherent paths due to the geomagnetic non-dipolar components ([Vestine et al., 1947](#); [Hillhouse and Cox, 1976](#); [Turner and Thompson, 1982](#); [Verosub, 1988](#); [Vigliotti, 2006](#)), particularly during the polarity reversals of the field.

Modeling the EMF means finding proper mathematical descriptions that account for the dispersion of the VGPs as the magnetic poles wander around the geographic poles. It also means evaluating the varying contributions of dipolar and non-dipolar components when we go back in time. In recent decades, good modeling has been achieved for the recent field ([Panovska et al., 2019](#)), but there are still many issues to elucidate regarding old fields. Furthermore, as the paleomagnetic database increases, more rigorous filters may be applied to the data, and better EMF models can be constructed.

Paleomagnetic measurements through sedimentary sections contribute significantly to cyclostratigraphy ([Strasser et al., 2006](#)). This term refers to identifying deposition cycles in sedimentary rocks, usually induced by the quasi-periodic oscillations in the Earth's orbital cycles of precession, obliquity, and eccentricity (Milankovitch cycles) on the global climate system over 10^4 - 10^6 years. The magneto-cyclostratigraphy has been increasingly used to refine the chronostratigraphic framework of sedimentary sections worldwide.

Since its early days in operation, the Laboratory of Paleomagnetism at Instituto de Astronomia, Geofísica e Ciências Atmosféricas of the University of São Paulo (IAG/USP) has invested in studying the secular variation of the paleomagnetic field and magnetostratigraphy of lava flow sequences ([Pacca and Hiodo, 1976](#); [Pacca and Ernesto, 1982](#); [Ernesto et al., 1979](#); [1988](#); [1990](#)) and contributed significantly to the world database of various ages. Nowadays, the PSV is explored in multiple aspects, and much effort is concentrated on understanding ancient times field behavior. The following sections will overview some of the leading research in the geomagnetic field behavior through time presently conducted at IAG/USP.

KINEMATICS OF THE VIRTUAL GEOMAGNETIC POLES

Paleomagnetic records from continuous sedimentary columns, mainly from lakes and oceans, are the best data source to investigate the long-term changes in the paleomagnetic field, both the secular variation and the polarity inversions. [Caminha-Maciél and Ernesto \(2020\)](#) examined VGPs from 20 ocean sedimentary cores widely distributed and with medium ($10 \text{ mm} \geq \text{rates} < 20 \text{ mm/kyr}$) to high ($\text{rates} \geq 20 \text{ mm/kyr}$) deposition rates. All cores cover the last ~ 1.2 My. This time interval includes the most recent polarity transition and various excursions (when the geomagnetic pole undergoes a significant drift towards the opposite hemisphere and then goes back without completing the reversal). A set of more than 40×10^3 VGPs was plotted together to reveal the shared kinematic characteristics during the Brunhes-Matuyama (BM) polarity transition ($\sim 783 \text{ kyr}$; [Mark et al., 2017](#)). The 2D histogram of all VGPs ([Figure 1](#)) shows the preferred sites the VGPs occupied during the Brunhes time, and its transition to the Matuyama

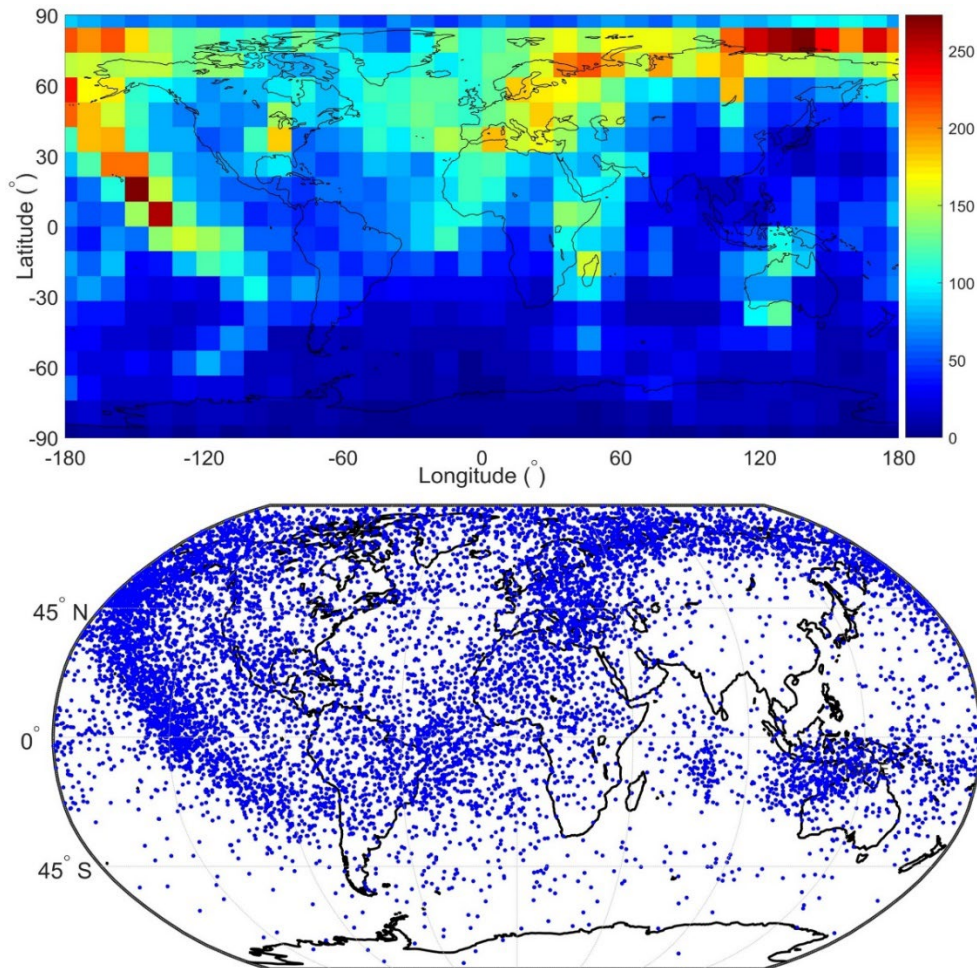


Figure 1: (Top) Density distribution of all investigated VGPs. The lateral bar is the counting scale. The bottom graphics represents the distribution of the VGPs from high-resolution core records (rates ≥ 20 mm/kyr). Modified from [Caminha-Maciél and Ernesto \(2020\)](#).

reversed chron. Although not clear, the longitudinal preferential paths advocated by [Clement \(1991\)](#) and [Lai et al. \(1991\)](#) on sediments and by [Hoffman \(1991\)](#) and [Love \(1998\)](#) on lavas are delineated on this figure over the Pacific realm and one over western Africa. However, a more exciting pattern appeared in the VGP distribution if only the high-resolution cores were considered ([Figure 1](#), bottom). The transitional latitudes, departing up to 45° from the equator, are preferentially over the Pacific. The VGP plots do not differentiate the N-S to S-N pathways during the various swings of the geomagnetic field. Instead, they only show the VGP density distribution or the preferable areas on the globe that reflect the deep Earth's conductivity characteristics.

The statistical approach demonstrated that some kinematics parameters might be extracted from the data. Mean velocities and accelerations of the VGPs are similar to those observed in recent times. The authors found mean rates of about $0.1^\circ/\text{yr}$ for normal, reversed

and transitional VGPs, even for those closer to the equator (within latitudes of 30° to -30°). Therefore, there is no clear evidence of faster movements of VGPs during transitions or excursions, although significant differences in the velocity azimuths may exist. For the normal field, azimuths concentrate at around 0° or 360° and around 180° for the reversed field, as expected. An east-west component was also detected but not as a relevant feature. [Figure 2](#) shows the mean acceleration as a function of the azimuth for the three polarity states – normal, reversed, and transitional. No significant differences were observed during the “stable” and transitional fields. The acceleration azimuths show variations from north-south to east-west depending on the field state, normal/reversed or transitional. Despite the possible inaccuracy in the magnetization record of sediments, the authors demonstrated that using an extensive database might be more adequate for investigating the kinematic parameters of the geomagnetic field on a statistical basis.

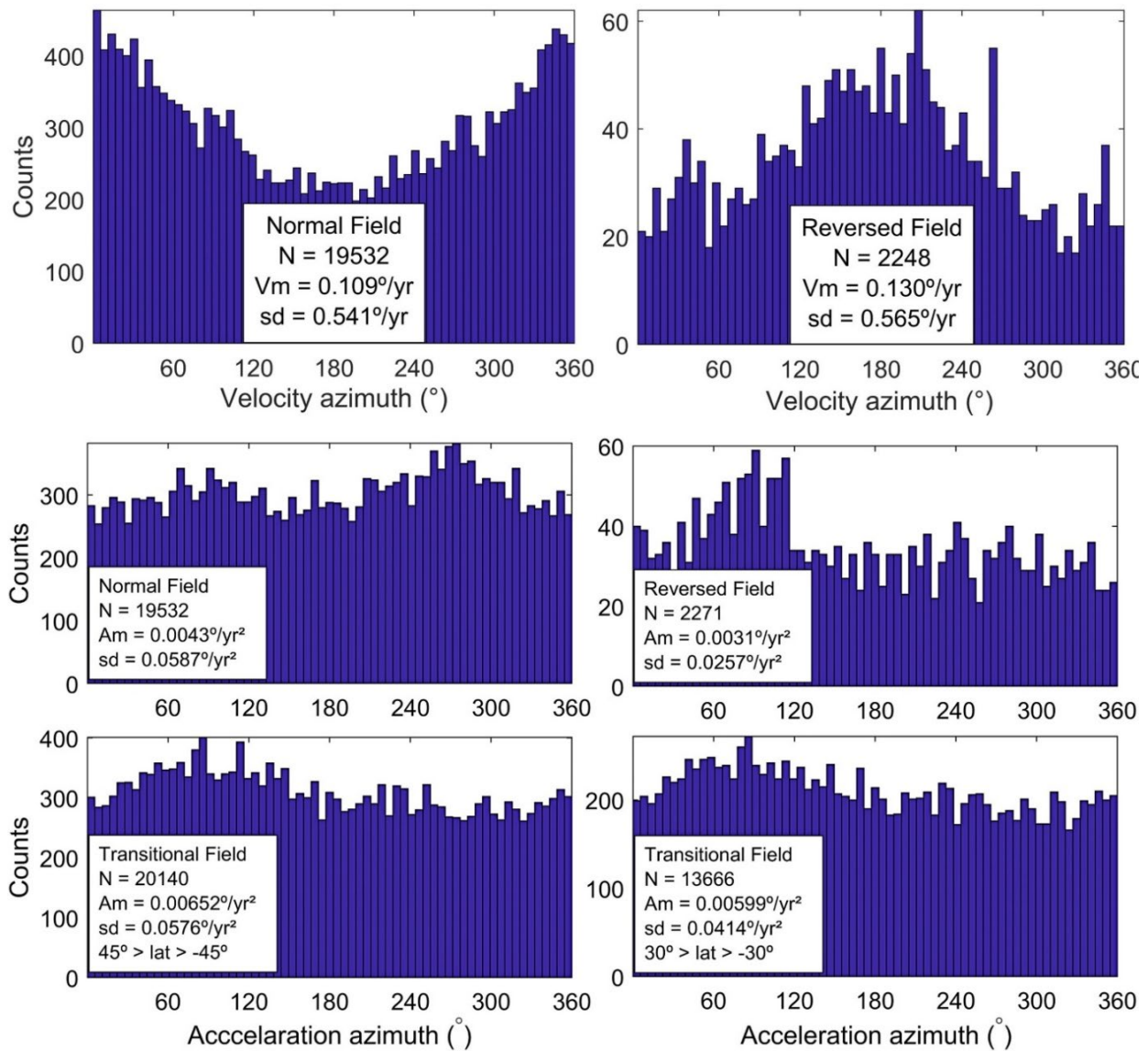


Figure 2: Histograms of the velocity and acceleration azimuths for the normal and reversed polarity VGPs. The bottom figures are the acceleration of the transitional VGPs considering two different latitude bands. N is the number of observations, Am is the mean velocity or acceleration, and sd is the standard deviation.

PSV MODELING DURING DIFFERENT TIME INTERVALS

In paleomagnetic studies, the PSV is expressed by the statistical scatter of the paleomagnetic directions or, more commonly, of the corresponding VGPs. Several models for the latitude (λ) variation of this angular dispersion (S_F) have been suggested, as summarized by Merrill et al. (1996) and [McElhinny and McFadden \(1997\)](#). [McFadden et al. \(1988\)](#) proposed model G, according to which the latitude variation of VGP scatter may be given by

$$S_F = \sqrt{a^2 + (b\lambda)^2}.$$

The shape parameters a and b represent the geomagnetic field's equatorially symmetric (quadrupolar) and antisymmetric (dipolar) components, respectively. This modeling approach was applied for different time intervals along the Phanerozoic ([McFadden et al., 1991](#)). [Figure 3](#) summarizes the fits of various compilations for different time intervals with varying rates of polarity change. The minimum rates correspond to the Permian-Carboniferous Reversed Superchron (PCRS or Kiaman; ~318-262 Ma; [Opdyke and Channell, 1996](#)) and the Cretaceous Normal Superchron (CNS; ~120-83 Ma; [He et al., 2012](#)). The PSV from periods of low reversal rates, as the CNS, has a relatively lower (higher) contribution

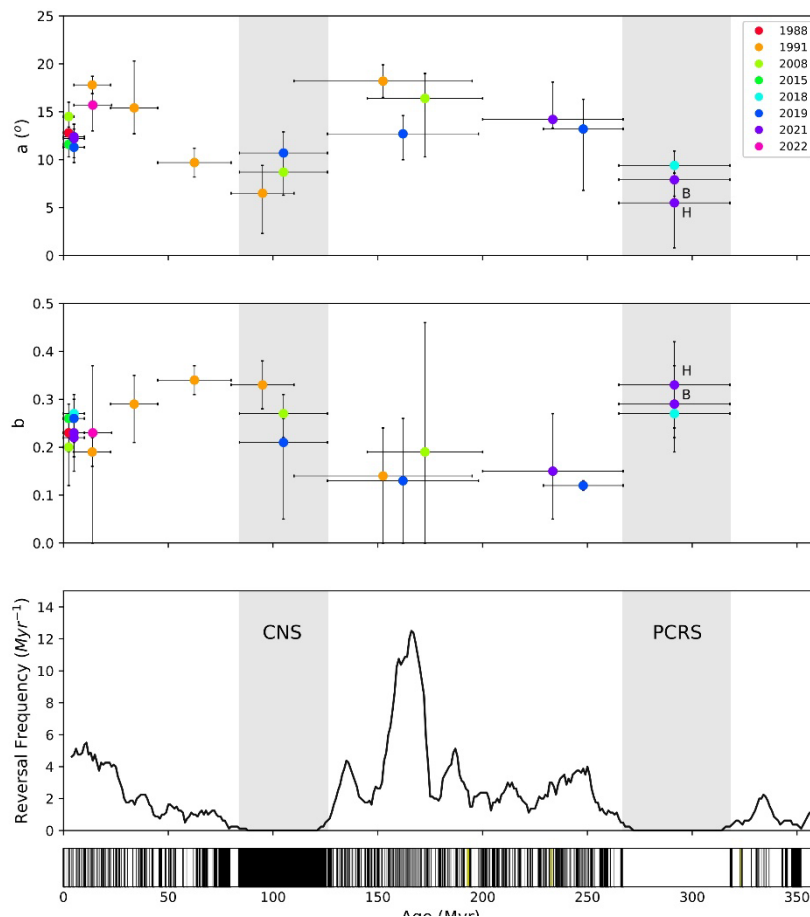


Figure 3: Model G shape parameters (a and b) according to various compilations and ages since the Carboniferous. [McFadden et al. \(1988, 1991\)](#); [Biggin et al. \(2008\)](#); [Johnson et al. \(2008\)](#); [Opdyke et al. \(2015\)](#); [Cromwell et al. \(2018\)](#); [Oliveira et al. \(2018\)](#); [Dobrovine et al. \(2019\)](#); [Sprain et al. \(2019\)](#); [Franco et al. \(2019\)](#); [Oliveira et al. \(2021\)](#); [Handford et al. \(2021\)](#); [Brandt et al. \(2021\)](#); [Engbers et al. \(2022\)](#). Average reversal frequency calculated with an 8 Ma sliding window ([Melott et al., 2018](#)) and geomagnetic polarity timescale (bottom) indicating the normal (black) and reversed (white) chrons.

of symmetric (antisymmetric) family contributors when compared with periods of higher reversal frequencies (e.g., the last 5 Ma and Jurassic). [Franco et al. \(2012a\)](#) analyzed the PSV record of the regular Rio do Sul rhythmites (Itararé Group, Paraná Basin) of the Permo-Carboniferous age and found a reduced VGP scatter for the correspondent paleolatitude of the rock unit. It was the first step for the first high-quality directional paleomagnetic database and evaluation of the (paleo)latitudinal variation of PSV for the PCRS ([Oliveira et al., 2018](#)). As a result, a remarkable similarity of (paleo)latitudinal dependence of angular VGP dispersion for both PCRS and CNS (lower VGP dispersion at low paleolatitudes and a prominent paleolatitudinal dependence). For a better understanding of the paleolatitudinal dependence of PSV during high reversal frequency intervals, [Franco et al. \(2019\)](#) studied the high geomagnetic reversal frequency interval Illawarra Hyperzone of Mixed Polarity (~266.7–228.7 Ma). This

study confirmed the similar behavior of the VGP dispersion pattern (with a low antisymmetric family contribution) for the Illawarra with the other high reversal frequency intervals, the Jurassic and the last 5 Ma. Noteworthy, the authors found an inverse correspondence between the relative contribution of the axial dipole field, given by the b/a ratio for the Model G shape parameters and the core-mantle boundary heat flux for the past 270 Myr ([Olson and Amit, 2015](#)).

Giant Gaussian Process modeling

The PSV models are generally based on the mathematical description of the scalar field potential (Ψ) in spherical harmonic functions where the magnetic field \mathbf{H} at any place out the Earth's core is $\mathbf{H} = -\mathbf{grad}(\Psi)$. The magnetic scalar potential for any geometry of magnetic source is an expansion of infinite spherical harmonic functions given by the Gauss coefficients (g_l^m, h_l^m):

$$\mathbf{H} = (H_\theta, H_\phi, H_r) = -\nabla\Psi = \left(-\frac{1}{r} \frac{\partial\Psi}{\partial\theta}, -\frac{1}{r\sin\theta} \frac{\partial\Psi}{\partial\phi}, -\frac{\partial\Psi}{\partial r} \right)$$

$$\Psi = \frac{r_a}{\mu_0} \sum_{l=1}^{\infty} \sum_{m=0}^l \left(\frac{r_a}{r} \right)^{l+1} (g_l^m \cos m\phi + h_l^m \sin m\phi) P_l^m(\cos\theta)$$

A commonly used family of statistical magnetic field models is based on a giant Gaussian process (GGP), a stochastic process according to which the Gauss coefficients can be accomplished from independent normal distributions. One of the most used GGP models (TK03; [Tauxe and Kent, 2004](#)) predicts an elongated distribution of the paleomagnetic directions. However, this model has been fitted to the recent field and did not account for the characteristic of a steady field like the PCRS field. [Oliveira et al. \(2018\)](#) drew attention to the VGP scatter during the PCRS and the last 5 Ma field. [Brandt et al. \(2019\)](#) also noticed that the reversed directions from the Paleozoic Mafra rhythmites (Paraná Basin) did not follow the expected elongated shape predicted by the TK03 model questioning the validity of the model for the PCRS. [Brandt et al. \(2020\)](#) adjusted their new GGP model BCE19 using an updated database ([Cromwell et al., 2018](#)) for the last 10 Ma. Furthermore, the compilation of a specific database for the PCRS (PDKRS is available at Magnetics Information Consortium - MagIC, <https://earthref.org/MagIC/16854>) allowed [Brandt et al. \(2021\)](#) to propose the first GGP model for the PCRS and evaluate the paleosecular

variation from a directional point of view.

Unlike Model-G, the GGP models can predict the Earth's surface direction distributions. They are based on the description of the field by spherical harmonics functions, so their temporal variation is described by the variation of Gaussian coefficients ($g_l^m(t), h_l^m(t)$). The main idea of the Gaussian process is that the random temporal sampling of each coefficient follows a normal distribution with a mean and a standard deviation. In this way, what defines a GGP model is a collection of means and standard deviations related to each of the Gaussian coefficients.

The pioneer CP88 model had all Gaussian coefficients with a null mean value, except for the g_1^0 and g_2^0 , which corresponds to a geocentric axial dipole and quadrupole, respectively. The standard deviation is $\sigma_l^2 = \frac{(c/a)^{2l} a^2}{(l+1)(2l+1)}$ where l is the coefficient degree, c/a is the ratio between the core and Earth radii (0.547), and α is a fitted constant. Therefore, only three parameters defined the CP88 model - $\overline{g_1^0}$, $\overline{g_2^0}$ and α . Other configurations of GGP models ([Table 1](#)) have been proposed, all based on a collection of means and standard deviations for all coefficients.

Table 1: Parameters of GGP-type models for various time intervals. Last 5 My: CP88 ([Constable and Parker, 1988](#)), and TK03 ([Tauxe and Kent, 2004](#)). Last 10 My: BCE19 ([Brandt et al., 2020](#)) and BB18.Z3 ([Bono et al., 2020](#)). Miocene: BB-M22 ([Engbers et al., 2022](#)). PCRS (KRSM, KRScovM, [Brandt et al., 2021](#)).

PARAMETER	CP88	TK03	BCE19	BB18.Z3	KRSM	KRSCOV M	BB-M22
AGE	0-5MY	0-5MY	0-10MY	0-10MA	PCRS	PCRS	MIOCENE
$\overline{g_1^0} (\mu T)$	-30.0	-18.0	-18.0	-22.04	28.9	28.9	-15.8
$\overline{g_2^0} (\mu T)$	-1.8	0.0	0.0	-0.65	0.0	0.0	0.0
$\overline{g_3^0} (\mu T)$	0.0	0.0	0.0	0.29	0.0	0.0	0.0
$\sigma_1^0 (\mu T)$				10.8			10.3
$\alpha (\mu T)$	27.7	7.3	6.7	12.25	8.8	10.6	12.33
β	-	3.8	4.2	2.82	3.8	3.1	2.2
COVARIANT	NO	NO	NO	YES	NO	YES	YES

The BCE19 ([Brandt et al., 2020](#)) is a simplified GGP model based on TK03 ([Tauxe and Kent, 2004](#)). This model, in turn, is based on a GAD time average field (only $\bar{g}_1^0 \neq 0$) and, beyond, another constant β defines all standard deviations. TK03 has the formula described by [Constable and Parker \(1988\)](#) for σ_l^2 , but the antisymmetric coefficients have more significant variance than the symmetric ones, amplifying the variation given by the dipolar field ($\sigma_l^2 = \frac{(c/a)^2 a^2 \beta^2}{(l+1)(2l+1)}$, for odd coefficients). Those modifications and simplifications introduced by the TK03 model helped to fit the last 5 My data by the results of the VGP scatter, which still needs to be solved with the CP88 model. As the magnetic field in a place is described by a linear combination of the Gaussian coefficients, normal distributions describe the orthogonal components of \mathbf{H} , which follows a 3D-Gaussian probability density function. The paleomagnetic data are only directional (declination and inclination) with no module. Therefore, the appropriate way of considering the field pdf is using the normalized version, that is, pdfs for unit vectors given by a GGP Model ([Constable and Parker, 1988](#); [Khokhlov et al., 2001, 2006](#)).

[Brandt et al. \(2020\)](#) contributed to finding a measure from directional paleomagnetic data that could theoretically determine using the probability distribution function (pdf) for unitary vectors from any GGP model. The theoretical determination avoids using random simulations of thousands of synthetic directions in the modeling process. This is time-consuming and always gives minor differences in the results (a method commonly used in modeling by VGP scatter).

This idea was not new, as the first proposed GGP model ([Constable and Parker, 1988](#)) already used the same methodology to calculate the pdf of unit vectors. However, the introduction of the β parameter ([Tauxe and Kent, 2004](#)), make it unfeasible to follow the original formulation. In the BCE19, the PSV is measured by the standard deviations (north-south, σ_N and east-west, σ_E) of the equal area coordinates (x_N, x_E) of the distributions rotated to the vertical ([Figure 4](#)). The advantages are: 1) the numerical determination is exact and faster than random sampling simulations; 2) the standard deviations (σ_N, σ_E) of the equal area coordinates of the rotated directions do not explode for higher values as it is the case of the standard deviations of declinations when distributions are near the poles (see [Figure 6](#) from [Constable and Parker, 1988](#)).

When it was published, the BCE19 was the best representation of the last 10 Ma PSV. However, a further step in modeling the geomagnetic field has been given by [Bono et al. \(2020\)](#), proposing another GGP model (BB18.Z3). The authors used the VGP scatter as a PSV measurement and considered the paleointensity data (PINT10, from PINT database, [Biggin et al., 2009](#); updated [Biggin et al., 2015](#)) for determining the mean \bar{g}_1^0 . [Brandt et al. \(2021\)](#) proposed a GGP model for the PCRS, the first for ages older than 10 Ma. The directional PSV indicated that the PCRS had a low paleosecular variation with approximately circular direction distributions (NE). For latitudes higher than 10°, directions are more concentrated and almost invariant, which is incompatible with the 10 Ma data ([Figure 5](#)). The intensity of the mean axial dipole coefficient (\bar{g}_1^0) was evaluated by the paleointensity results of PCRS age from the PINT database ([Table 1](#)). Two versions of GGP models were fitted to the Kiaman directional PSV results. The first one (KRSM in [Table 1](#)) followed the formulation from [Tauxe and Kent \(2004\)](#), where only three parameters define the GGP model (\bar{g}_1^0, α and β) and the Gaussian coefficients are considered independent variables. The second one (KRScovM, [Table 1](#) and [Figure 5](#)) followed the same formulation but using the correlations determined from dynamo simulations according to [Bono et al. \(2020\)](#). The best model for the Kiaman PSV found, considering the least 2 misfit ([Brandt et al., 2021](#)), is the covariant type. However, the almost circular shape of the directional data allows a reasonable doubt – does it represent the real low Kiaman PSV, or is the dispersion dominated by the experimental noise, and could the PSV be even lower?

FINDING HARMONIC COMPONENTS IN PALEOMAGNETIC TIME SERIES

The magnetostratigraphy of the Serra Geral Formation ([Ernesto et al., 1990](#)), the flood basalts of the Paraná Basin in southern Brazil, revealed the continuous changes in the paleomagnetic directions that could be associated with the PSV record. [Pacca and Ernesto \(1982\)](#) adjusted sinusoidal components to declination and inclination sequences from some magma flow piles. This result motivated [Caminha-Macieli and Ernesto \(2013\)](#) to search for harmonic components in the Serra Geral series even though the data are not on a temporal basis. To overcome this difficulty, they analyzed the VGP

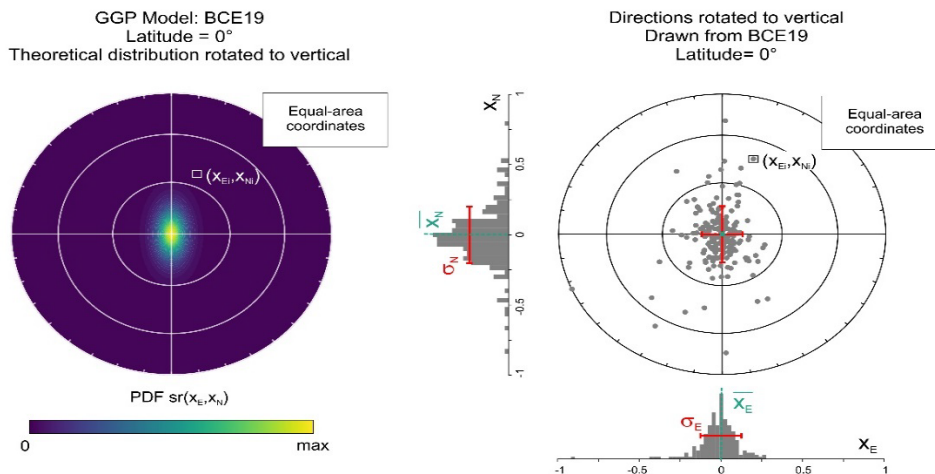


Figure 4: Left: theoretical probability density function rotated to the vertical predicted by the BCE19 model. Right: two hundred directions drawn from the BCE19 model at the Equator with the expected direction (declination=0°, inclination=0°) rotated to the vertical, and the estimative of the mean (x_N , x_E) and standard deviations (σ_N , σ_E) of equal area coordinates (x_N , x_E).

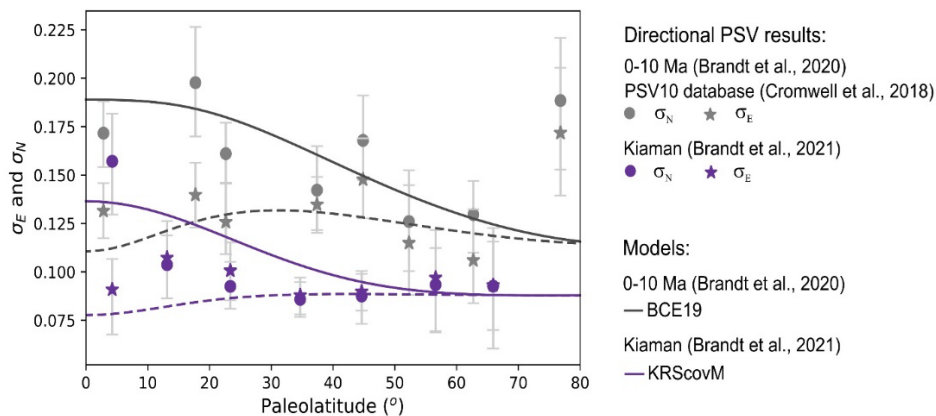


Figure 5: Directional PSV results and GGP models for 0-10 Ma (grey lines and symbols) and PCRS (purple lines and symbols).

latitudes as a function of longitude. As the data sequences are irregularly sampled, the periodogram was the best choice to perform the spectral analysis. The authors developed a modified version of the Lomb-Scargle periodogram (Lomb, 1976; Scargle, 1982) to incorporate a Bayesian combination of information. The result was a method of spectral analysis that combines all the individual spectra. This combination of information approach is a stacking-like procedure reducing noise and highlighting features that may not be sufficiently clear in a particular spectrum. The combinations are in two different modes – correspond to the ‘OR’ and ‘AND’ operations over all states of information (function describing the different estimates for each frequency) – resembling the union and intersection of sets (Tarantola and Mosegaard, 2000).

Mathematically, these operations can be related to the sum (OR) and product (AND) of these states of information after normalization by total bandwidth.

Despite the differences in sampling density and length of the Serra Geral series, the new method could identify common harmonic features in the datasets. However, the physical meaning of the wavelengths still needs to be deciphered. A friendly version of the method called LSTperiod (Caminha-Maciel and Ernesto, 2019) performs spectral analysis of irregularly sampled time series. It evaluates the reliability of the determined wavelengths with various statistics and tools. Cabot and Laughlin (2022) discussed the efficiency of stacked periodograms and compared the LSTperiod with their method finding similar performance in both cases.

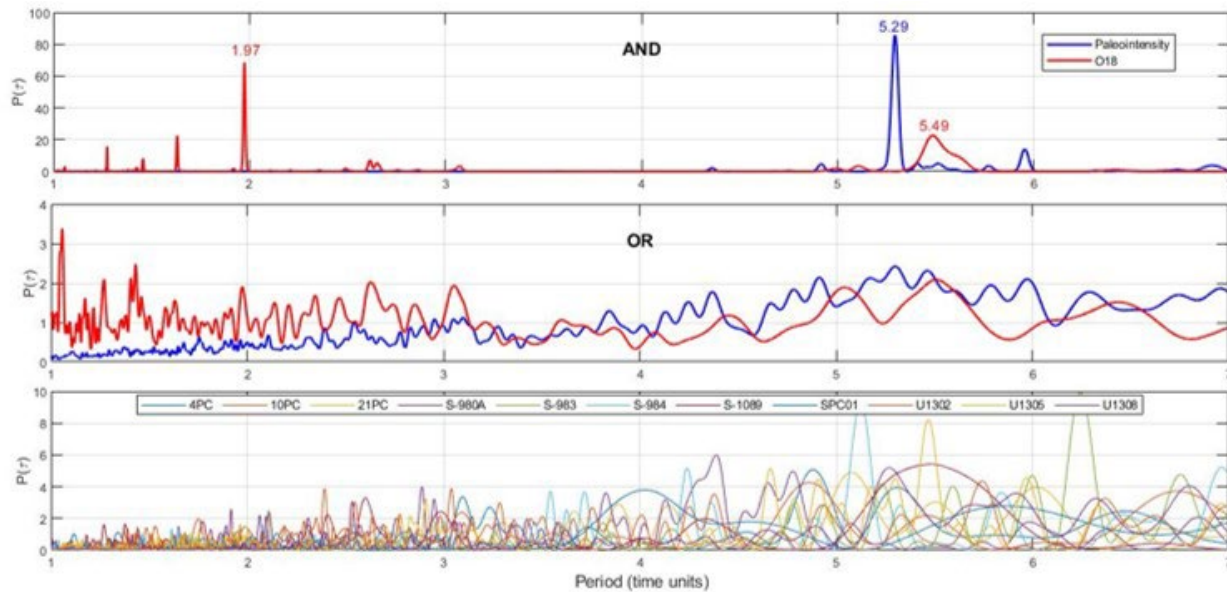


Figure 6: The LST periodograms for each of the paleointensity series (bottom). The combined OR and AND spectra for the paleointensity (blue line) and $\delta^{18}\text{O}$ (red line) series. The $\delta^{18}\text{O}$ series are from the same or nearby cores.

The use of the LSTperiod may be illustrated by analyzing paleointensity records. Marine sedimentary columns show longer and continuous records, but the paleointensity is not absolute because the magnetization process in sediments does not establish a direct relationship with the magnetizing field, as in volcanic rocks. The relative paleointensity (RPI) from sedimentary rocks is usually obtained by normalizing the natural remanent magnetization (NRM) intensity of the sedimentary rocks by the imparted anhysteretic remanent magnetization (ARM). This normalization produces a parameter that allows data correlation from different sedimentary cores.

The RPI (NRM/ARM) series from ten marine sedimentary cores were downloaded from Pagaea and ODP data repositories. The sites are from similar latitudes (45° - 60°) in the North and South Atlantic Oceans and covering the last 100 kyr were analyzed (Siqueira, 2021). The AND spectrum (Figure 6), the Bayesian combination of the components after normalization, gave a sharp peak at $T = 5.29$ kyr, which corresponds to the period of a phenomenological control on the RPI data. The OR spectrum (Figure 6) represents the arithmetical average of all the spectrum features in the individual series (Figure 6).

However, as climatic variations control sedimentation, examining the isotope variation in the sediments is an essential proxy for climate change. The LSTperiod of the $\delta^{18}\text{O}$ data from the same cores (980, 983, 984, and 1089) or nearby sites (database from Lisiecki and

Ravmo, 2005) showed a dominant peak at $T = 1.97$ kyr and only a slight indication of a harmonic signal at $T = 5.49$ kyr (AND spectrum; Figure 6). The 5.29 kyr cycle could be a subharmonic of the shortest orbital cycle. However, if the climate is the determinant factor for the paleointensity variability, the prominent peak of 1.98 kyr in the $\delta^{18}\text{O}$ spectra should also be present in the magnetic data.

Figure 7a illustrates the performance of the LSTperiod method in adjusting the harmonic components to the original data. The detected 5.29 kyr signal in the RPI data is in phase in some series (Figure 7b), independent of their located hemisphere. The 5.29 kyr signal in the RPI records is in the suborbital range. Orbital cycles are longer, from 10^4 to 10^6 kyr (Milankovich cycles; Hinnov and Hilgen, 2012). The Atlantic climate cyclicity throughout the Holocene seems not exclusively a consequence of solar forcing but depends on multiple factors, including ocean circulation (Debret et al., 2007). A period of 1.768 kyr in ^{10}Be and ^{14}C was reported by McCracken et al. (2013) for the interval 40-9400 BP, which does not differ significantly from the period of 1.98 kyr in the AND spectrum. The ~ 3.37 kyr period reported by Santos et al. (2013) in the equatorial $\delta^{18}\text{O}$ did not appear, but the isotopic content may vary depending on the latitude (Zhao et al., 2021). In conclusion, the differences in the RPI and $\delta^{18}\text{O}$ spectra are not undisputable evidence to attribute an internal cause to the 5.3 kyr period in the RPI data, but it is an unprecedented observation using a new analytical approach.

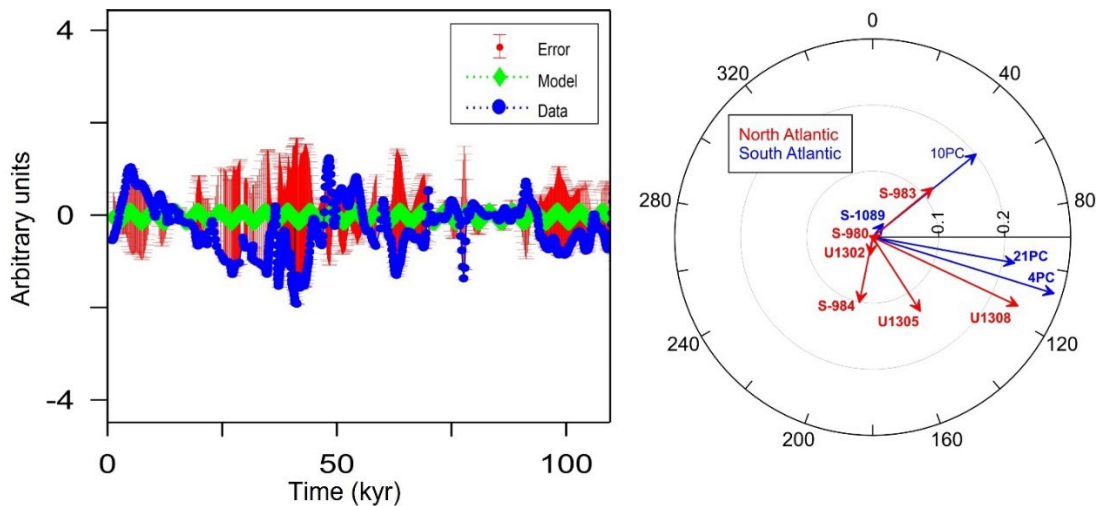


Figure 7: a) Comparative plots of the obtained $T = 5.29$ kyr model, the associated error, and original data for the U1308 series; b) phases and amplitudes of the $T = 5.29$ kyr signal in the RPI series.

Magneto-Cyclostratigraphy

In Brazil, the pioneering effort to determine quasi-periodic processes in sedimentary successions took place at the IAG/USP in the 1980s. [Ernesto and Pacca \(1981\)](#) evaluated the Itu rhythmite section consisting of stratified lithological pairs (LPs) of sandstone/siltstone and siltstone/argillite. Despite the centimeter-scale pair thicknesses, these rhythmites were supposed to be varvites (e.g., [Rocha-Campos et al., 1981](#)) as they resembled the Pleistocene varves. The spectral analysis applied to the pair thickness and the magnetic data (susceptibility and directional data) indicated periodicities mainly in the range of 5.5-22 units considering annual sedimentation. However, the varve hypothesis was dismissed (e.g., [Caetano-Chang and Ferreira, 2006](#)) due to the abnormal sedimentation rates for an annual deposition and other sedimentological features consistent with rhythmites. A new project was envisaged to provide better constraints on the rhythmite timescales.

A magnetostratigraphic survey was conducted on the Itu (State of São Paulo) and the Itaú quarry (Rio do Sul formation, State of Santa Catarina), both having the same lithological characteristics but positioned in different levels of the Permo-Carboniferous stratigraphic column of the Paraná Basin. [Franco et al. \(2011\)](#) observed that the magnetic declinations were greater than 16° between and 4° within LPs, therefore, much exceeding the annual changes in declination of the geomagnetic field (of the order of only $0.5^\circ/\text{yr}$) even considering the paleomagnetic experimental errors.

Both the Itu and Rio do Sul sections gave characteristic remanent magnetization (ChRM) for more than 100 LPs from each sequence ([Franco et al., 2012a](#)), and cyclostratigraphic analyses were performed on the directional ChRM and the bulk magnetic susceptibility with a sampling rate of ~ 2 cm for both sections ([Franco et al., 2012b](#)). The results pointed to a low-frequency spectral content in the stratigraphy domain consistent with the spectral ratios predicted for Milankovitch cycles during the Permian ([Berger et al., 1992](#)), therefore incompatible with the annual cyclicity hypothesis. Additionally, a remarkable sub-orbital-scale record was identified as compatible with the abrupt climate changes during the late Quaternary and suggestive of the 2.4 kyr solar cycle and Bond cycles. These last cycles refer to the ice rafting events due to climatic fluctuations, as [Bond et al. \(2001\)](#) described. Such results indicate that those millennial-scale climate change processes could be prevalent over geological time.

The magneto-cyclostratigraphy for the Itaú quarry rhythmites also helped better position both sections within the Permo-Carboniferous stratigraphic column, allowing the calculation of a paleomagnetic reference pole for South America. Later, another Permo-Carboniferous rhythmite section (Mafra Formation, State of Santa Catarina) went through magneto-cyclostratigraphic evaluations ([Brand et al., 2019](#)). This time, the lithological pairs were thinner (up to a few centimeters), and the astronomical calibration was fundamental to setting the timespan encompassed by the ~ 120 LPs. This control was

necessary to eliminate the secular variation in the calculation of the paleomagnetic pole and was also successfully applied for a paleomagnetic investigation of the Late Paleozoic Mafra Fm. rhythmites (Brandt et al., 2019).

Franco and Hinnov (2013) explored the efficiency of the K1 maximum axis of the anisotropy of magnetic susceptibility as a paleoclimatic proxy for the rhythmite sequences obtaining the same low- to high-frequency spectral content verified in the thickness, bulk susceptibility and ChRM direction datasets. In a climatically controlled sedimentary system, the current-induced fabric may be responsible for the anisotropy of susceptibility depending on the mineralogical contributions.

In short, magneto-cyclostratigraphy is becoming a critical tool in paleomagnetism and paleosecular variation studies, as it helps constrain sedimentary column's elapsed time. It also has the potential to improve the chronostratigraphic frameworks at the unprecedented temporal resolution, compatible with the scale of astronomical cycles, as discussed in a recent paper by Leandro et al. (2022).

Concluding Remarks

The modeling of the geomagnetic field depends on the familiarity of its temporal and spatial characteristics. Furthermore, as it is a highly dynamic field, it is necessary to investigate time intervals in which the magnetic field showed contrasting behaviors, such as lower and high rates of polarity inversion. Much progress has been made in this knowledge over the last 50 years, but there is still much to investigate. The search for harmonic fluctuations in the field and its relationship with climate change is now one of the frontier topics. In this sense, cyclo-magnetostratigraphy has risen as a whole line of investigation, contributing to the refinement of chronostratigraphy.

In this work, we seek to highlight some lines of investigation that contribute to improving the knowledge of the field and that are being developed at IAG/USP and other Brazilian research centers.

ACKNOWLEDGMENTS

This work is the result of many years of research that counted on the involvement of many collaborators. It also benefited from financial support from the Brazilian funding agencies, FAPESP, CNPq, FINEP, CAPES and FAPERJ. In addition, the authors are grateful to the two

anonymous reviewers for their valuable contributions to improving the paper. Thanks are also given to the editors for managing this paper.

REFERENCES

- Berger, A., M.F. Loutre, and J. Laskar, 1992, Stability of the astronomical frequencies over the Earth's history for paleoclimate studies: *Science*, **255**, 560–566, doi: [10.1126/science.255.5044.560](https://doi.org/10.1126/science.255.5044.560)
- Biggin, A.J., D.J. Van Hinsbergen, C.G. Langereis, G.B. Straathof, and M.H. Deenen, 2008, Geomagnetic secular variation in the Cretaceous Normal Superchron and in the Jurassic: *Phys. Earth Planet. Int.*, **169**, 3–19, doi: [10.1016/j.pepi.2008.07.004](https://doi.org/10.1016/j.pepi.2008.07.004).
- Biggin, A.J., and C.G. Langereis, 2009, The intensity of the geomagnetic field in the late-Archaeon: New measurements and an analysis of the updated IAGA palaeointensity database: *Earth, Planets and Space*, **6**, 9–22, doi: [10.1186/BF03352881](https://doi.org/10.1186/BF03352881).
- Biggin, A.J., E.J. Piispa, L.J. Pesonen, R. Holme, G.A. Paterson, T. Veikkolainen, and L. Tauxe, 2015, Palaeomagnetic field intensity variations suggest Mesoproterozoic inner-core nucleation: *Nature*, **526**, 245–248, doi: [10.1038/nature15523](https://doi.org/10.1038/nature15523).
- Bond, G., B. Kromer, J. Beer, R. Muscheler, and M.N. Evans, W. Showers, S. Hoffmann, R. Lott-Bond, I. Hajdas and G. Bonani, 2001, Persistent solar influence on North Atlantic climate during the Holocene: *Science*, **294**, 2130–2136, doi: [10.1126/science.1065680](https://doi.org/10.1126/science.1065680).
- Bono, R.K., A.J. Biggin, R. Holme, C.J. Davies, D.G. Meduri, and J. Bestard, 2020, Covariant giant Gaussian process models with improved reproduction of palaeosecular variation: *G-Cubed*, **21**, e2020GC008960, doi: [10.1029/2020GC008960](https://doi.org/10.1029/2020GC008960).
- Brandt, D., M. Ernesto, C. Constable, D.R. Franco, L.C. Weinschutz, P.O.C. Rodrigues, L. Hinnov, P. Jaqueto, P.B. Strauss, and J. Feinberg, 2019, New late Pennsylvanian paleomagnetic results from Paraná Basin (southern Brazil) and the validity of the recent Giant Gaussian Process model for the Kiaman Superchron: *J. Geophys. Res.*, **124**, doi: [10.1029/2018JB016968](https://doi.org/10.1029/2018JB016968).
- Brandt, D., C. Constable, and M. Ernesto, 2020, Giant Gaussian process models of geomagnetic paleosecular variation: a directional outlook: *Geophys. J. Intern.*, **222**, 1526–1541, doi: [10.1093/gji/ggaa258](https://doi.org/10.1093/gji/ggaa258).
- Brandt, D., M. Ernesto, and C. Constable, 2021, Consistent and contrasting aspects of the geomagnetic field across epochs with distinct reversal frequencies revealed by modeling the Kiaman Superchron: *G-Cubed*, **22**, e2021GC009866, doi: [10.1029/2021GC009866](https://doi.org/10.1029/2021GC009866).

- Brunhes, B., 1906, Recherches sur la direction d'aimantation des roches volcaniques: *Journal de Physique Théorique et Appliquée*, **5**, 705–724, doi: [10.1051/jphysstap:019060050070500](https://doi.org/10.1051/jphysstap:019060050070500).
- Butler, F.B., 1992, *Paleomagnetism: Magnetic domains to geologic terranes*: Blackwell Scientific Publications, Oxford, 319 p.
- Cabot, S.H.C., and G. Laughlin, 2022, Stacked periodograms as a probe of exoplanetary populations: *The Astronomical Journal*, **163**, 206, 9 pp., doi: [10.3847/1538-3881/ac54b5](https://doi.org/10.3847/1538-3881/ac54b5).
- Caetano-Chang, M.R., and S.M. Ferreira, 2006, Ritmitos de Itu: Petrografia e Considerações paleodeposicionais: *Geociências*, **25**, 345–358.
- Caminha-Maciel, G., and M. Ernesto, 2013, Characteristic wavelengths in VGP trajectories from magnetostratigraphic data of the Early Cretaceous Serra Geral lava piles, southern Brazil, *in* Jovane, L., E. Herrero-Bervera, L. Hinnov, B.A. Housen, Eds., *Magnetic methods and the Timing of Geological Processes: The Geological Society of London, Special Publications*, **373**, 293–307, doi: [10.1144/SP373.15](https://doi.org/10.1144/SP373.15).
- Caminha-Maciel, G., and M. Ernesto, 2019, LSTperiod Software: Spectral Analysis of Multiple Irregularly Sampled Time Series: *Annals of Geophys.*, **62**, doi: [10.4401/ag-7923](https://doi.org/10.4401/ag-7923).
- Caminha-Maciel, G., and M. Ernesto, 2020, Kinematics of the virtual geomagnetic poles during the Brunhes-Matuyama times, *in* Tema E., A. Di Chiara, E. Herrero-Bervera, Eds., 2020, *Geomagnetic Field Variations in the Past: New Data, Applications and Recent Advances: Geological Society of London, Special Publications*, **497**, 193–204, doi: [10.1144/SP497-2019-80](https://doi.org/10.1144/SP497-2019-80).
- Clement, B.M., 1991, Geographical distribution of transitional VGPs: evidence for non-zonal equatorial symmetry during the Matuyama-Brunhes geomagnetic reversal: *Earth Planet. Sci. Lett.*, **104**, 48–58, doi: [10.1016/0012-821X\(91\)90236-B](https://doi.org/10.1016/0012-821X(91)90236-B).
- Constable, C.G., and R.L. Parker, 1988, Statistics of the geomagnetic secular variation for the past 5 m.y.: *J. Geophys. Res.*, **93**, B10, 11569–11581, doi: [10.1029/JB093iB10p11569](https://doi.org/10.1029/JB093iB10p11569).
- Cromwell, G., C. Johnson, L. Tauxe, C. Constable, and N. Jarboe, 2018, PSV10: A global data set for 0–10 Ma time-averaged field and paleosecular variation studies: *Geochemistry, Geophysics, Geosystems*, **19**, 1533–1558, doi: [10.1002/2017GC007318](https://doi.org/10.1002/2017GC007318).
- Debret, M., V. Bout-Roumazeilles, F. Grousset, M. Desmet, J.F. McManus, N. Masse, D. Sebag, J.-R. Petit, Y. Copard, and A. Trentesaux, 2007, The origin of the 1500-year climate cycles in Holocene North-Atlantic records: *Clim. Past*, **3**, 569–575, doi: [10.5194/cp-3-569-2007](https://doi.org/10.5194/cp-3-569-2007).
- Dobrovine, P.V., T. Veikkolainen, L.V. Pesonen, E. Piispa, S. Ots, A.V. Smirnov, E.V. Kulakov, and A.J. Biggin, 2019, Latitude dependence of geomagnetic paleosecular variation and its relation to the frequency of Magnetic reversals: observations from the Cretaceous and Jurassic: *G-Cubed*, **20**, 1240–1279, doi: [10.1029/2018GC007863](https://doi.org/10.1029/2018GC007863).
- Engbers, Y.A., R.K. Bono, and A. Biggin, 2022, PSVM: A global database for the Miocene indicating elevated paleosecular variation relative to the last 10 Myrs: *G-Cubed*, **23**, e2022GC010480, doi: [10.1029/2022GC010480](https://doi.org/10.1029/2022GC010480).
- Ernesto, M., F.Y. Hiodo, and I.G. Pacca, 1979, Estudo paleomagnético de sequência de derrames basálticos da Formação Serra Geral em Santa Catarina: *Anais Acad. Brasil. Ciênc.*, **51**, 328–332.
- Ernesto, M., and I.G. Pacca, 1981, Spectral analysis of Permocarboneous geomagnetic variation data from glacial rhythmites: *J. R. Astron. Soc.*, **67**, 641–647, doi: [10.1111/j.1365-246X.1981.tb06943.x](https://doi.org/10.1111/j.1365-246X.1981.tb06943.x).
- Ernesto, M., and I.G. Pacca, 1988, Paleomagnetism of the Parana Basin flood volcanics, southern Brazil, *in* Piccirillo, E.M. and A.J. Melfi, Eds., *The Mesozoic flood volcanism of the Parana Basin: petrogenetic and geophysical aspects*, IAG/USP, 229–255.
- Ernesto, M., I.G. Pacca, F.Y. Hiodo, and A.J.R. Nardy, 1990, Paleomagnetism of the Mesozoic Serra Geral Formation, southern Brazil: *Phys. Earth Planet. Int.*, **64**, 153–175, doi: [10.1016/0031-9201\(90\)90035-V](https://doi.org/10.1016/0031-9201(90)90035-V).
- Evans, M.E., and G.S. Hoyer, 2007, Testing the GAD throughout geological time: *Earth, Planets and Space*, **59**, 697–701, doi: [10.1186/BF03352732](https://doi.org/10.1186/BF03352732).
- Franco, D.R., and L.A. Hinnov, 2013, Anisotropy of magnetic susceptibility and sedimentary cycle data from Permo-Carboniferous rhythmites (Paraná Basin, Brazil): a multiple proxy record of astronomical and millennial scale palaeoclimate change in a glacial setting: *Geological Society, London, Special Publications*, **373**, 355–374, doi: [10.1144/SP373.11](https://doi.org/10.1144/SP373.11).
- Franco, D.R., L.A. Hinnov, and M. Ernesto, 2011, Spectral analysis and modeling of microcyclostratigraphy in late Paleozoic glaciogenic rhythmites, Paraná Basin, Brazil: *G-Cubed*, **12**, Q09003, doi: [10.1029/2011GC003602](https://doi.org/10.1029/2011GC003602).
- Franco, D.R., M. Ernesto, C.F. Ponte-Neto, L.A. Hinnov, T.S. Berquó, J.D. Fabris, and C.A. Rosière, 2012a, Magnetostratigraphy and mid-paleolatitude VGP dispersion during the Permo-Carboniferous Superchron: results from Paraná Basin (southern Brazil) rhythmites: *Geophys. J. Int.*, **191**, 993–1014, doi: [10.1111/j.1365-246X.2012.05670.x](https://doi.org/10.1111/j.1365-246X.2012.05670.x).
- Franco, D.R., L.A. Hinnov, and M. Ernesto, 2012b, Millennial-scale climate cycles in Permian-Carboniferous rhythmites: Permanent feature throughout geologic time?: *Geology*, **40**, 19–22, doi: [10.1130/G32338.1](https://doi.org/10.1130/G32338.1).
- Franco, D.R., W.P. Oliveira, F.B.V. Freitas, D. Takahashi, C.F. Ponte-Neto, and I.M.C. Peixoto,

- 2019, Paleomagnetic evidence for inverse correspondence between the relative contribution of the axial dipole field and CMB heat flux for the past 270 Myr: *Scientific Reports*, **9**, 282, doi: [10.1038/s41598-018-36494-x](https://doi.org/10.1038/s41598-018-36494-x).
- Gradstein, F.M., J.G. Ogg, and F.J. Hilgen, 2012, On the Geologic Time Scale: *Newsletters on Stratigraphy*, **45**, 171–188, doi: [10.1127/0078-0421/2012/0020](https://doi.org/10.1127/0078-0421/2012/0020).
- Handford, B.T., A.J. Biggin, M.M. Haldan, and C.G. Langereis, 2021, Analyzing Triassic and Permian geomagnetic paleosecular variation and the implications for ancient field morphology: *G-Cubed*, **22**, e2021GC009930, doi: [10.1029/2021GC009930](https://doi.org/10.1029/2021GC009930).
- He, H., C. Deng, P. Wang, Y. Pan, and R. Zhu, 2012, Toward age determination of the termination of the Cretaceous Normal Superchron: *G-Cubed*, **13**, Q02002, doi: [10.1029/2011GC003901](https://doi.org/10.1029/2011GC003901).
- Hillhouse, J., and A. Cox, 1976, Brunhes-Matuyama polarity transition: *Earth Planet. Sci. Lett.*, **2**, 51–64, doi: [10.1016/0012-821X\(76\)90025-X](https://doi.org/10.1016/0012-821X(76)90025-X).
- Hinnov, L., and F.J. Hilgen, 2012, Cyclostratigraphy and astrochronology, in Gradstein F., J. Ogg, G. Ogg, and D. Smith, Eds., *A Geologic Time Scale*: Elsevier, Amsterdam, 63–83, doi: [10.1016/b978-0-444-59425-9.00004-4](https://doi.org/10.1016/b978-0-444-59425-9.00004-4).
- Gradstein, F.M., Ogg J.G., Schmitz M.D., and Ogg G.M., 2012, *The Geologic Time Scale*: Elsevier, doi: [10.1016/C2011-1-08249-8](https://doi.org/10.1016/C2011-1-08249-8).
- Hoffman, K.A., 1991, Long-lived transitional states of the geomagnetic field and the two dynamo families: *Nature*, **354**, 273–277, doi: [10.1038/354273a0](https://doi.org/10.1038/354273a0).
- Johnson, C.L., C.G. Constable, L. Tauxe, R. Barendregt, L.L. Brown, R.S. Coe, P. Layer, V. Mejia, Opdyke N.D., Singer B.S., H. Staudigel, and D.B. Stone, 2008, Recent investigations of the 0–5 Ma geomagnetic field recorded by lava flows: *G-Cubed*, **9**, doi: [10.1029/2007GC001696](https://doi.org/10.1029/2007GC001696).
- Khokhlov, A., G. Hulot, and J. Carlot, 2001, Towards a self-consistent approach to palaeomagnetic field modelling: *Geophys. J. Int.*, **145**, 157–171, doi: [10.1111/j.1365-246X.2001.01386.x](https://doi.org/10.1111/j.1365-246X.2001.01386.x).
- Khokhlov, A., G. Hulot, and C. Bouligand, 2006, Testing statistical palaeomagnetic field models against directional data affected by measurement errors: *Geophys. J. Int.*, **167**, 635–648, doi: [10.1111/j.1365-246X.2006.03133.x](https://doi.org/10.1111/j.1365-246X.2006.03133.x).
- Laj, C.A., A. Mazaud, M. Weeks, M. Fuller, and E. Herrero-Bervera, 1991, Geomagnetic reversal paths: *Nature*, **351**, 447, doi: [10.1038/351447a0](https://doi.org/10.1038/351447a0).
- Langereis, C.G., W. Krijgsman, G. Muttoni, and M. Menning, 2010, Magnetostratigraphy - concepts, definitions, and applications: *Newsletter on Stratigraphy*, **43**, 3, 207–233, doi: [10.1127/0078-0421/2010/0043-0207](https://doi.org/10.1127/0078-0421/2010/0043-0207).
- Leandro, C.G., J.G. Savian, M.V.L. Kochhann, D.R. Franco, R. Coccioni, F. Frontalini, S. Gardin, L. Jovane, M. Figueiredo, L.R. Tedeschi, L. Janikian, R.P. Almeida, and R.I.F. Trindade, 2022, Astronomical tuning of the Aptian stage and its implications for age recalibrations and paleoclimatic events: *Nature Commun.*, **13**, 2941, doi: [10.1038/s41467-022-30075-3](https://doi.org/10.1038/s41467-022-30075-3).
- Lisiecki, L.E., and M.E. Raymo, 2005, Pliocene-Pleistocene stack of globally distributed benthic stable Oxygen isotope records: PANGAEA [dataset], doi: [10.1594/PANGAEA.704257](https://doi.org/10.1594/PANGAEA.704257).
- Lomb, N.R., 1976, Least-squares frequency-analysis of unequally spaced data: *Astrophys. Space Sci.*, **39**, 447–462, doi: [10.1007/BF00648343](https://doi.org/10.1007/BF00648343).
- Love, J.J., 1998, Paleomagnetic volcanic data and geometric regularity of reversals and excursions: *J. Geophys. Res.*, **1031**, 12435–12452, doi: [10.1029/97JB03745](https://doi.org/10.1029/97JB03745).
- Mark, D.F., P.R. Renne, R.C. Dymock, V.C. Smith, J.E. Simon, L.E. Morgan, R.A. Staff, B.S. Ellis, and N.J.G. Pearce, 2017, High-precision $^{40}\text{Ar}/^{39}\text{Ar}$ dating of Pleistocene tuffs and temporal anchoring of the Matuyama-Brunhes boundary: *Quaternary Geochron.*, **39**, 1–23, doi: [10.1016/j.quageo.2017.01.002](https://doi.org/10.1016/j.quageo.2017.01.002).
- McCracken, K.G., J. Beer, F. Steinhilber, and J. Abreu, 2013, A Phenomenological Study of the Cosmic Ray Variations Over the Past 9400 Years: *Solar Physics*, **286**, 609–627, doi: [10.1007/s11207-013-0265-0](https://doi.org/10.1007/s11207-013-0265-0).
- McElhinny, M.W., and P.L. McFadden, 1997, Palaeosecular variation over the past 5 Myr based on a new generalized database: *Geophys. J. Int.*, **131**, 240–252, doi: [10.1111/j.1365-246X.1997.tb01219.x](https://doi.org/10.1111/j.1365-246X.1997.tb01219.x).
- McFadden, P.L., R.T. Merrill, and M.W. McElhinny, 1988, Dipole/quadrupole family modeling of paleosecular variation: *J. Geophys. Res.*, **93**, 11,583–11,588, doi: [10.1029/JB093iB10p11583](https://doi.org/10.1029/JB093iB10p11583).
- McFadden, P.L., R.T. Merrill, M.W. McElhinny, and S. Lee, 1991, Reversals of the Earth's magnetic field and temporal variations of the dynamo families: *J. Geophys. Res.*, **96**, 3923–3933, doi: [10.1029/90JB02275](https://doi.org/10.1029/90JB02275).
- Melott, A., A. Pivarunas, J. Meert, and B. Lieberman, 2018, Does the planetary dynamo go cycling on? Re-examining the evidence for cycles in magnetic reversal rate: *Int. J. Astrobiology*, **17**, 44–50, doi: [10.1017/S1473550417000040](https://doi.org/10.1017/S1473550417000040).
- Merrill, R.T., M.W. McElhinny, and P.L. McFadden, 1996, *The Magnetic Field of the Earth: Paleomagnetism, the Core, and the Deep Mantle*. International Geophysics Series, **63**, Academic Press, 531 p.
- Oliveira, W.P., D.R. Franco, D. Brandt, M. Ernesto, C.F. Ponte-Neto, X. Zhao, F.B.V. Freitas, and R.S. Martins, 2018, Behavior of the paleosecular variation

- during the Permian-Carboniferous Reversed Superchron and comparisons to the low reversal frequency intervals since Precambrian times: *Geochemistry, Geophysics, Geosystems*, **19**, 1035–1048, doi: [10.1002/2017GC007262](https://doi.org/10.1002/2017GC007262).
- Oliveira, W.P., G.A. Hartmann, F. Terra-Nova, D. Brandt, A.J. Biggin, Y.A. Engbers, R.K. Bono, J.F. Savian, D.R. Franco, R.I.F. Trindade, and T.R. Moncinhatto, 2021, Paleosecular Variation and the Time-Averaged Geomagnetic Field Since 10 Ma: G-Cubed, **22**, e2021GC010063, doi: [10.1029/2021GC010063](https://doi.org/10.1029/2021GC010063).
- Olson, P., and H. Amit, 2015, Mantle superplumes induce geomagnetic superchrons: *Frontiers in Earth Science*, **3**, 38, doi: [10.3389/feart.2015.00038](https://doi.org/10.3389/feart.2015.00038).
- Opdyke, D.N., and J.E.T. Channell, 1996, *Magnetic Stratigraphy*: Elsevier, eBook ISBN: 9780080535722.
- Opdyke, N.D., D.V. Kent, D.A. Foster, and K. Huang, 2015, Paleomagnetism of Miocene volcanics on Sao Tome: Paleosecular variation at the Equator and a comparison to its latitudinal dependence over the last 5 Myr: *Geochemistry, Geophysics, Geosystems*, **16**, 3870–3882, doi: [10.1002/2015GC005901](https://doi.org/10.1002/2015GC005901).
- Pacca, I.G., and F.Y. Hiodo, 1976, Paleomagnetic analysis of Mesozoic Serra Geral basaltic lava flows in Southern Brazil: *An. Acad. Brasil. Ciênc.*, **48** (Supl.), 207–214.
- Pacca, I.G., and M. Ernesto, 1982, Utilização da variação paleosseccular e de reversões do campo geomagnético para medidas de tempo decorrido entre eventos magmáticos sucessivos: *Proceedings of the XXXII Congresso Brasileiro de Geologia*, Salvador, BA, Brazil, **4**, 1621–1628.
- Panovska, S., M. Korte, and C.G. Constable, 2019, One hundred thousand years of geomagnetic field evolution: *Reviews of Geophysics*, **57**, 1289–1337, doi: [10.1029/2019RG000656](https://doi.org/10.1029/2019RG000656).
- Rocha-Campos, A.C., M. Ernesto, and D. Sundaram, 1981, Geological, palynological and paleomagnetic investigations on Late Paleozoic Varvites from the Paraná Basin, Brazil: 3^o Simpósio Regional de Geologia, Curitiba, PR, Brazil, *Actas*, **2**, 162–175.
- Santos, TP., D.R. Franco, C.F. Barbosa, A.L. Belem, T. Dokken, and A.L.S. Albuquerque, 2013, Millennial-to centennial-scale changes in sea surface temperature in the tropical South Atlantic throughout the Holocene: *Palaeogeography, Palaeoclimatology, Palaeoecology*, **392**, 1–8, doi: [10.1016/j.palaeo.2013.08.019](https://doi.org/10.1016/j.palaeo.2013.08.019).
- Scargle, J.D., 1982, *Studies in astronomical time-series analysis II. Statistical aspects of spectral analysis of unevenly spaced data*: *Astrophys. J.*, **263**, 835–853, doi: [10.1086/160554](https://doi.org/10.1086/160554).
- Siqueira, T.C.G.B., 2021, *Variações temporais de longo período do campo geomagnético: análise espectral da paleointensidade relativa*: Monography, UnED, CEFET/RJ, Petrópolis, RJ, Brazil, 52 p.
- Sprain, C.J., A.J. Biggin, C.J. Davies, R.K. Bono, and D.G. Meduri, 2019, An assessment of long duration geodynamo simulations using new paleomagnetic modeling criteria (Q_{pm}): *Earth Planet. Sci. Lett.*, **526**, 115758, doi: [10.1016/j.epsl.2019.115758](https://doi.org/10.1016/j.epsl.2019.115758).
- Strasser, A., F.J. Hilgen, P.H. Heckel, 2006, Cyclostratigraphy - concepts, definitions, and applications: *Newsl. Stratigr.*, **42**, 75–114, doi: [10.1127/0078-0421/2006/0042-0075](https://doi.org/10.1127/0078-0421/2006/0042-0075).
- Tarantola, A., and K. Mosegaard, 2000, *Mathematical basis for physical inference*: Cornell University Library, New York, [arXiv:math-ph/0009029v1](https://arxiv.org/abs/math-ph/0009029v1), Access on: July 7, 2022.
- Tauxe, L., and D.V. Kent, 2004, A simplified statistical model for the geomagnetic field and the detection of shallow bias in paleomagnetic inclinations: Was the ancient magnetic field dipolar?, *in* Channell, J.E.T., D.V. Kent, W. Lowrie, and J.G. Meert, Eds., *Timescales of the Paleomagnetic Field*: AGU, Washington, D.C., **145**, 101–115, doi: [10.1029/145GM08](https://doi.org/10.1029/145GM08).
- Turner, G.M., and R. Thompson, 1982, Detransformation of the British geomagnetic secular variation record for Holocene times: *Geophys. J.R. Astron. Soc.*, **70**, 789–792, doi: [10.1111/j.1365-246X.1982.tb05983.x](https://doi.org/10.1111/j.1365-246X.1982.tb05983.x).
- Vestine, E.H., L. Laporte, C. Cooper, I. Lange, and W.C. Hendrix, 1947, *Description of the Earth's main magnetic field and its secular change, 1905-1945*: Carnegie Inst. Wash. Publ., Washington, D.C., 578.
- Verosub, K.L., 1988, Geomagnetic secular variation and the dating of Quaternary sediments *in* Easterbrook, D.J., Ed., *Dating Quaternary Sediments*: *Geol. Soc. America Special Papers*, **227**, 123–138, doi: [10.1130/SPE227-p123](https://doi.org/10.1130/SPE227-p123).
- Vigliotti, L., 2006, Secular variation record of the Earth's magnetic field in Italy during the Holocene: constraints for the construction of a master curve: *Geophys. J. Int., Geomagnetism, Rock Magnetism and Palaeomagnetism*, **165**, 414–429, doi: [10.1111/j.1365-246X.2005.02785.x](https://doi.org/10.1111/j.1365-246X.2005.02785.x).
- Zhao, X., W. Soon, and V.M. Herrera, 2021, Holocene Millennial-Scale Solar Variability and the Climatic Responses on Earth: *Universe*, **7**, 36, doi: [10.3390/universe7020036](https://doi.org/10.3390/universe7020036).

Ernesto, M.; Brandt, D.; Franco, D.R.; Caminha-Maciel, G.: All authors idealized the work and provided revisions on their research topics.

Received on August 31, 2022 / Accepted on April, 19, 2023